Theoretical Evaluation of Solar Assisted Desiccant Cooling System for a Small Meeting-Hall

Khalid Ahmed Joudi
Prof. of Mechanical engineering
Department of Mechanical Engineering
College of Engineering
University of Baghdad

Hussam Hikmat Jabbar
Department of Mechanical Engineering
College of Engineering
University of Baghdad
hussam_alziadi86@yahoo.com

ABSRTACT

　　The performance of a solar assisted desiccant cooling system for a meeting-hall located in the College of Engineering/University of Baghdad was evaluated theoretically. The system was composed of four components; a solar air heater, a desiccant dehumidifier, a heat exchanger and an evaporative cooler. A computer simulation was developed by using MATLAB to assess the effect of various design and operating conditions on the performance of the system and its components. The actual weather data on recommended days were used to assess the load variation and the system performance during those days.

　　The radiant time series method (RTS) was used to evaluate the hourly variation of the cooling load. Four operation modes were employed for performance evaluation. A 100 % ventilation mode and 3 recirculation modes, 30 % , 60 % and 100 % recirculation of room air. The concept of variable air volume was employed as a control strategy over the day, by changing the supply airflow rate to match the variation in the cooling load.

　　The results showed that the reduction in moisture content at regeneration temperatures from 55 $^{\circ}$C to 75 $^{\circ}$C lead to adequate removal of the high latent load in the meeting-hall. Also, the 30 % recirculation of return air resulted in comfortable indoor conditions satisfying the ventilation requirements for most periods of system operation. In addition, the COP of the system was high compared with the conventional vapor compression system. It varied from 1 to 13, when considering solar energy used to regenerate the desiccant material as free energy.

KEYWORDS: Desiccant cooling system, Radiant time series, Variable air volume.

دراسة نظرية لتقييم منظومة تبريد امتزازي تعمل بمساعدة الطاقة الشمسية لتكييف قاعة إجتماعات صغير

الخلاصة

　　تم تقييم اداء منظومة التبريد ألإمتزازية التي تعمل بمساعدة الطاقة الشمسية وتطبيقها على قاعة اجتماعات صغيرة تقع في كلية الهندسة/جامعة بغداد. تحتوي المنظومة على أربعة أجزاء: المجمع الشمسي والمجفف الدوار و المبادل الحراري و المبرد التبخيري. وقد تم تطوير برنامج محاكاة بإستخدام ال(ماتلاب) للمنظومة في مختلف ظروف التصميم و التشغيل ومعرفة تأثيرها على أداء ألمنظومة و مكوناتها. أستخدمت بيانات ألطقس الفعلية على أيام معينة من السنة لتقييم ألتغير في حمل التبريد و أداء المنظومة خلال تلك الايام.

　　أستخدمت طريقة (RTS) لتقييم التغير في حمل التبريد للقاعة خلال ساعات النهار. تم تشغيل المنظومة بأربع طرق تشغيل لتقييم أدائها.الطريقة الأولى هي طريقة التهوية 100 % والطرق الأخرى هي إعادة تدوير 30 % ، 60 % و 100 % من الهواء الراجع على التوالي. أستخدم مفهوم تدفق الهواء المتغير كإسلوب سيطرة على المنظومة لتغطي حمل التبريد المتغيير خلال النهار وذلك بتغيير معدل تدفق الهواء المجهز للحيز المكيف.

أظهرت النتائج إن الإنخفاض في نسبة الرطوبة عند درجة حرارة إعادة تنشيط تتراوح من 55 درجة مئوية الى 75 درجة مئوية. أدت الى إزالة جيدة للحمل الكامن في قاعة الاجتماعات. كذلك أظهرت النتائج ان تشغيل المنظومة مع تدوير الهواء الراجع من الحيز المكيف بنسبة 30 % كانت كافية لتوفير ظروف راحة لمعظم ساعات تشغيل المنظومة. بالأضافة الى ذلك فأن معامل أداء المنظومة عالي جدا (1 – 13) مقارنة بأجهزة تكييف الهواء الإنضغاطية التقليدية عند إعتبار الطاقة الشمسية التي تستخدم لاعادة تنشيط مادة التجفيف طاقة مجانية.

1. INTRODUCTION:

Cooling is important in space conditioning of most buildings in hot and warm climates and in large buildings in cooler climates. Cooling load and availability of solar radiation are approximately in phase. Three classes of systems can accomplish solar air conditioning: absorption cycles, desiccant cycles and solar-mechanical processes. Within these classes, there are many variations, using continuous or intermittent cycles, various temperature ranges of operation, different collectors...etc.

The desiccant dehumidification solar assisted air conditioning systems are finding increasing applications for humidity control in commercial and institutional buildings, such as supermarkets, schools, hotels, theaters and hospitals. **Daou et. al. [2006]** predicted the principal underlying the operation of desiccant cooling systems and their actual technological applications and feasibility of the desiccant cooling in different climates. Evaluating the performance of a solar assisted heating and desiccant cooling system by a computer simulation program for a domestic two-story residence was carried out by **Joudi and Dhaidan[2001]**. They developed a computer simulation to assess the effect of various designs and operating conditions on the performance of the system and its components. **Mittal et. al. [2007]** uses an artificial roughness on a surface to enhance the rate of heat transfer to fluid flow in the duct of a solar air heater. **Ammari [2003]** presented a mathematical model for computing the thermal performance of a single pass flat-plate solar air heater. He investigated the effect of volume airflow rate, collector length and spacing between the absorber and bottom plates on the thermal performance of the solar air heater. **Varun et. al. [2007]** investigated the effect of a number of geometries of roughness elements on the heat transfer and friction

characteristics of solar air heater ducts. **Mohammad [1983]** studied the performance of a V-corrugate solar air heater in Basra. Experimental measurements had been made for the air   mass flow rate and the temperature difference between the outlet and inlet temperatures and for the temperature distribution of the absorber plate. **Moneer [1997]** found that the average optimum tilt angle for May, June, July and August in Baghdad was 10° and changing this angle by $\pm10^o$ reduces the useful energy gained by only 2% . In another study, **Joudi and Dhaidan [2001]** found that the shading effect on the collector array is negligible in summer due to the small tilt angle in this season.

Zhang et. al. [2003] developed a one-dimensional coupled heat and mass transfer model of a rotary dehumidifier to predict the temperature and humidity profiles and to analyze and verify its performance with experimental data. They found that the desiccant wheel can have a high effectiveness of dehumidification if the regeneration temperature and the regeneration air velocity are high. **Kodama et. al. [2001]** proposed an effective prediction to estimate the optimal rotation speed and performance of a rotary absorber, in which simultaneous enthalpy and humidity changes are dealt with separately by visualizing change of state of product or exhaust air on a psychometric chart. **Nia et. al. [2006]** presented a model for a desiccant wheel used for dehumidifying the ventilation air of an air conditioning system. Simple correlations for the outlet air conditions of humidity and temperature of air through the wheel as a function of the physically measurable input variables were presented. The variables were the rotational speed, humidity ratio, and outdoor temperature entering the dehumidifier, velocity of air, solids thickness, regeneration

temperature and hydraulic diameter of the channel.

Evaporative cooling systems are of two types: indirect and direct. Indirect evaporative coolers lower the inlet ambient air temperature at constant moisture content. Thus, the cooling is sensible. Direct evaporative coolers introduce moisture into the inlet air stream, and cool the air stream adiabatically. An indirect system can be coupled with a direct system to give a maximum cooling effect. **Camargo et. al. [2005]** present the basic principles of the evaporative cooling process for human thermal comfort. **Joudi and Mehdi [2000]** conducted a study into the application of the indirect evaporative cooling in fulfillment of the variable cooling load of a typical Iraqi dwelling. The application was evaluated through a systematic

simulation, along with a comparison between two arrangements of an indirect-direct evaporative cooling system. Their results showed that indirect evaporative cooling would result in a comfortable indoor condition for most periods of system operation. The potential energy saving by replacing the conventional refrigeration system by an evaporative system was shown to be 75 % by **Datta et. al. [1987].** It was stated that the comfort afforded by an indirect evaporative system is superior to that achieved by direct evaporative system. **El-Dessouky et. al. [2004]** made an experimental rig of two-stage evaporative cooling unit. **Heidarinejad et. al. [2009]** predicted the cooling performance of a two-stage indirect/direct evaporative cooling system. The system was experimentally investigated in various simulated climatic conditions.

Variable-air-volume (VAV) system varies its supply air volume flow rate to match the reduction of space load during part-load operation. Variable-air-volume system was first introduced by **Urban [1969]** in the 1960s. It has a considerable advantage in energy saving over the constant-air-volume system

In this work, the desiccant cycle is studied. The cycle consist of four components, these are a solar collector, a desiccant dehumidifier wheel, a heat exchanger and an evaporative cooler. The target is to find out a suitable desiccant cooling system for a meeting-hall in the University of Baghdad. Four modes of operation were studied.

A computer program was built up using MATLAB program to simulate those operation modes. Then a comparison between the performances of these operation modes was compared to find the better mode that satisfies this type of application. Also, many parameters including ambient temperature, regeneration temperature, and inlet water temperature to the heat exchanger were investigated. The cooling load calculating method that was used to estimate the cooling load of the meeting hall is the Radiant Time Series (RTS). This method is the most recent cooling load calculation procedure introduced by **ASHRAE[2009].**

The MATLAB program and its language is used in this work for computer programming. The computation is composed of two main programs and a number of subprograms. These subprograms are coupled with each other and with the main program by FUNCTION commands. Fig.1-a and Fig.1-b show the flow chart for the two main program and there subprograms.

2. THEORY:

The radiant time series method (RTS) is a simplified method for performing design cooling load calculations that is derived from the heat balance (HB) method **ASHRAE[2009]**.It effectively replaces all other simplified (non-heat-balance) methods, such as the transfer function method TFM, the cooling load temperature difference/cooling load factor CLTD/CLF method, and the total equivalent temperature difference/time averaging TETD/TA method.

The RTS method was developed to offer a method that is rigorous, yet does not require iterative calculations, and that quantifies each component's contribution to the total cooling load.

2.1 RTS procedures:

The general procedure for calculating cooling load for each load component (lights, people, walls, roofs, windows, appliances, etc.) with RTS is as follows:

1. Calculate 24 h profile of component heat gains for the design day (for conduction, first account for conduction time delay by applying conduction time series).

2. Split heat gains into radiant and convective parts.
3. Apply appropriate radiant time series to radiant part of heat gains to account for time delay in conversion to cooling load.
4. Sum convective part of heat gain and delayed radiant part of heat gain to determine cooling load for each hour for each cooling load component.

After calculating cooling loads for each component for each hour, sum those to determine the total cooling load for each hour

and select the hour with the peak load for design of the air-conditioning system.

2.2 Calculating Conductive Heat Gain Using Conduction Time Series (CTS):

In the RTS method, conduction through exterior walls and roofs is calculated using conduction time series (CTS). Wall and roof
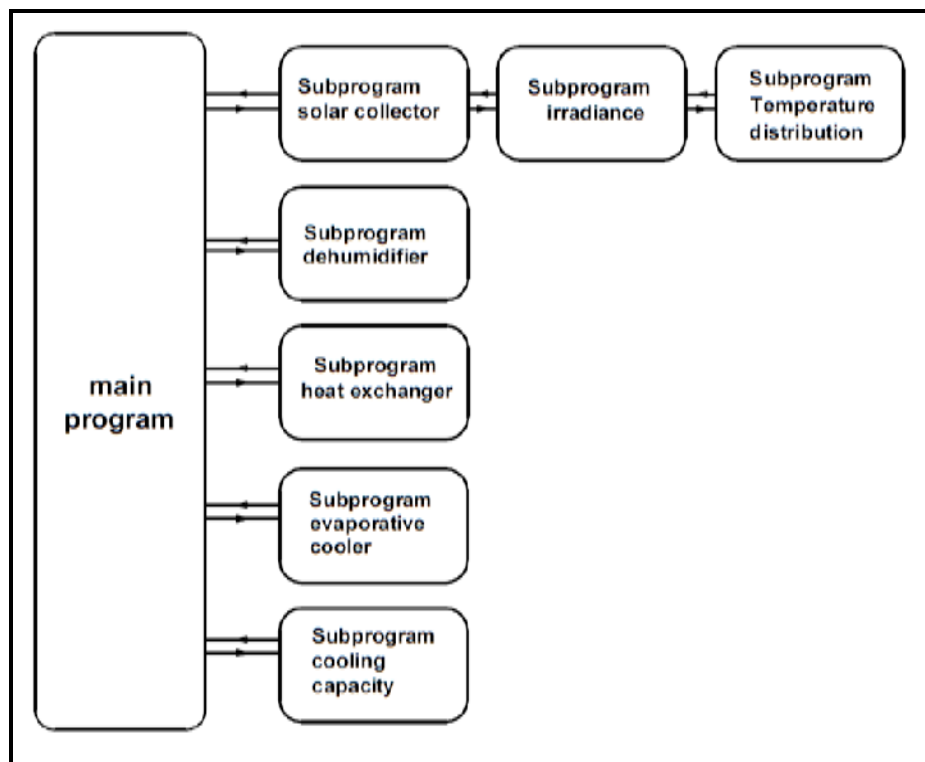
Fig.1-a The block diagram of the solar system performance program
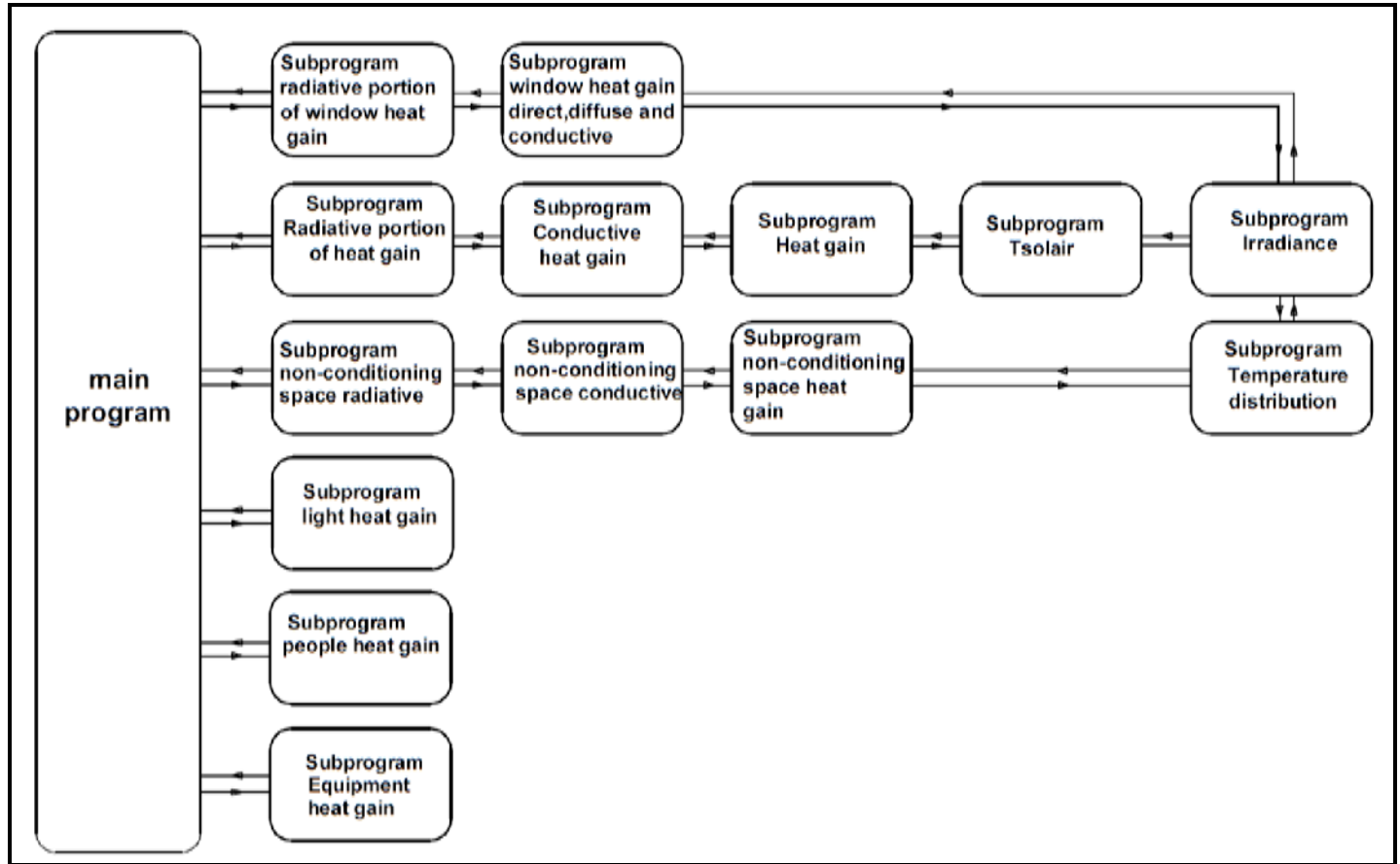
Fig.1-b The block diagram of the cooling load calculation program.

conductive heat input at the exterior is defined by the familiar conduction equation as:

$$q_{i,\theta-n} = U \, A \, (T_{sol} - T_r) \qquad (1)$$

Conductive heat gain through walls or roofs can be calculated using conductive heat inputs for the current hour, past 23 h, and conduction time series:

$$q_\theta = c_0 q_{i,\theta} + c_1 q_{i,\theta-1} + c_2 q_{i,\theta-2} + c_3 q_{i,\theta-3} + \cdots + c_{23} q_{i,\theta-23}$$

$$(2)$$

Where

q_θ = hourly conductive heat gain for the surface, W

$q_{i,\theta}$ = heat input for the current hour

$q_{i,\theta-n}$ = heat input n hours ago

c_0, c_1, etc. = conduction time factors

Conduction time factors for representative wall and roof types are included in **ASHRAE[2009]** tables. Those values were derived by first calculating conduction transfer

functions for each example wall and roof construction. Assuming steady-periodic heat input conditions for design load calculations allows conduction transfer functions to be reformulated into periodic response factors. The periodic response factors were further simplified by dividing the 24 periodic response factors by the respective overall wall or roof U-factor to form the conduction time series (CTS). The conduction time factors can then be used in Equation (2) and provide a way to compare time delay characteristics.

2.3 Calculating Cooling Load:

The hourly conductive heat gain can be separated into two parts, convective and

radiative. The convective portion converts to cooling load immediately and the radiative portion converts to cooling loads according to the following equation:

$$Q_{r,\theta} = r_0 q_{r,\theta} + r_1 q_{r,\theta-1} + r_2 q_{r,\theta-2} + r_3 q_{r,\theta-3} + \cdots + r_{23} q_{,\theta-23}$$

(3)

where

$Q_{r,\theta}$ = radiant cooling load Qr for current hour θ, W

$q_{r,\theta}$ = radiant heat gain for current hour, W
$q_{r,\theta-n}$ = radiant heat gain n hours ago, W
r_0, r_1, etc. = radiant time factors,

The radiant cooling load for the current hour, which is calculated using RTS, is added to the convective portion to determine the total cooling load for that component for that hour. Heat gains from people, light and equipment are convective to the space immediately. Therefore, they will be separated to convection heat gain and radiant heat gain each by its fraction of convection or radiation and then the radiant time series is applied to the radiant portions. Most designers do not include infiltration in cooling load calculations for commercial buildings and assume positive pressure for buildings under study.

For fenestration heat gain, the following equations are used:
Direct beam solar heat gain q_b:

$$q_b = AI_b SHGC(\theta)IAC(\theta,\Omega)$$

(4)

Diffuse solar heat gain q_d:

$$q_d = A(I_d + I_r)<SHGC>_D IAC_D$$

(5)

Where
SHGC(θ) = beam solar heat gain coefficient as a function of incident angle θ, its value varies from 0.81 to 0.73 when incident angle θ varies from 0° to 90°, for uncoated single glazing 6 mm thickness.
$<SHGC>_D$ = diffuse solar heat gain coefficient (also referred to as hemispherical SHGC); its value is 0.73 .

IAC($\theta.\Omega$) = indoor solar attenuation coefficient for beam solar heat gain coefficient = 1.0 if no inside shading device
IAC_D = indoor solar attenuation coefficient for diffuse solar heat gain coefficient = 1.0 if not inside shading device.

Conductive heat gain q_c:

$$q_c = U A (T_{out} - T_r)$$

(6)

Total fenestration heat gain Q:

$$Q = q_b + q_d + q_c$$

(7)

Fig.2 shows a plan of the meeting hall under study. It seats 100 occupants and the main exterior wall faces north. It is constructed of Iraqi standard building materials.
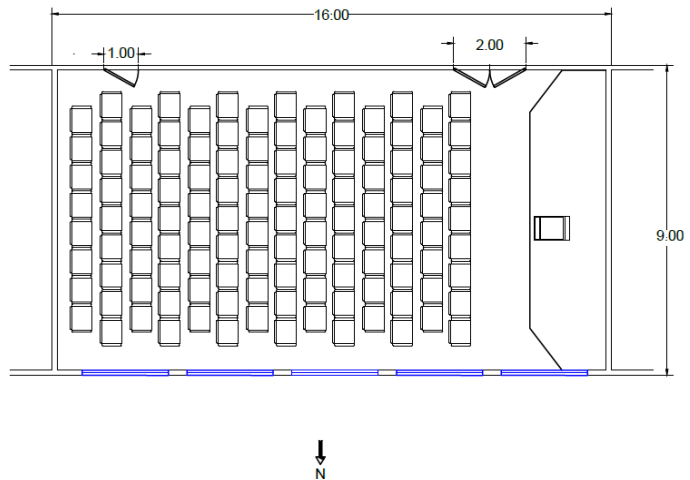

Fig.2 Schematic diagram for the meeting hall.

2.4 Open Cycle Desiccant Cooling System:

Fig.3-a and Fig.3-b show a schematic diagram of a ventilation cycle desiccant cooling system and its psychrometric representation respectively. While, Fig.4-a and Fig.4-b show a schematic diagram of the recirculation mode desiccant cooling system and the psychrometric representation respectively.

In steady state, the useful energy gain of a collector is the difference between the absorbed solar radiation and the thermal losses given by **Duffie and Beckman [2006]** is:

$$q_u = (\tau\alpha)\, I_t - U_l(T_p - T_a) \qquad (8)$$

Where $(\tau\alpha)$ is the optical losses. $(\tau\alpha)I_t$ is the absorbed energy by the collector. The term $U_l(T_p-T_a)$ is the thermal losses. The value of U_l varies with solar radiation during the hours of the day.

It is convenient that the useful energy gain is calculated as a function of inlet fluid temperature:

$$q_u = F_R\,[(\tau\alpha)I_t - U_l(T_{in}-T_a)] \qquad (9)$$

Where, F_R is the heat removal factor which is defined as the ratio of actual useful energy gain of collector to the useful energy gain if the entire absorber plate surface where at the inlet fluid temperature. F_R is given as;

$$F_R = \frac{G\,C_p}{U_l}[1 - \exp(\frac{F'U_l}{G\,C_p})] \qquad (10)$$

The performance of a solar air heater is expressed by the collection efficiency which is defined as:

$$\eta = \frac{q_u}{I_t} \qquad (11)$$

For simulation, the honeycomb desiccant dehumidifier wheel was used. This type of desiccant contains small channels shaped like honeycomb cells. The channels are coated from the inside by silica gel. For simplicity, the desiccant wheel is divided into two equal

sections: the adsorbing section and the regeneration section (desorption of water vapor). The regeneration and adsorption air streams are in a counter flow arrangement. The analysis is based on the following assumptions stated by Nia **et.al. [2006]**:

1. Axial heat conduction and water vapor diffusion in the air.
2. Axial molecular diffusion within the desiccant is negligible.
3. There are no radial temperature or moisture content gradients in the adsorbent matrix.
4. Hysteresis in the sorption isotherm for the desiccant coating was neglected and the heat of sorption was assumed constant.

5. The channels that make up the wheel are identical with constant heat and mass transfer surface areas.
6. The matrix thermal and moisture properties are constant.
7. The channels are considered adiabatic and impermeable.
8. The mass and heat transfer coefficients are constant.
9. The adsorption heat per kilogram of adsorbed water is constant.
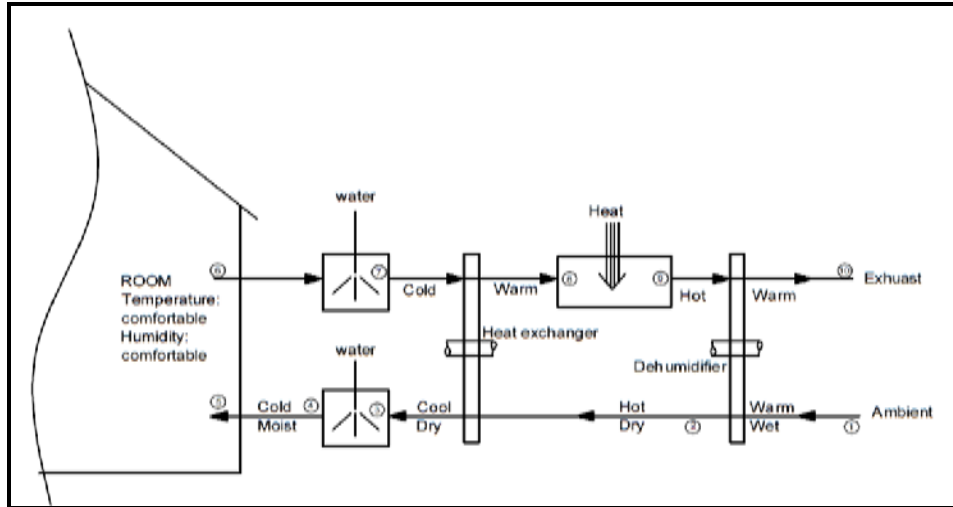10.   The carry over between two airflows is neglected.
11.

Fig.3-a Schematic diagram of a ventilation cycle desiccant cooling system.
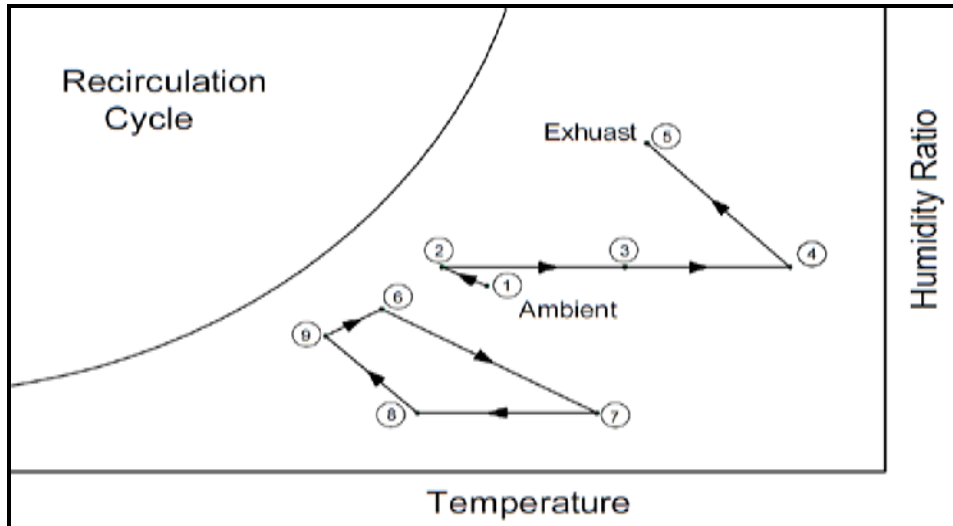

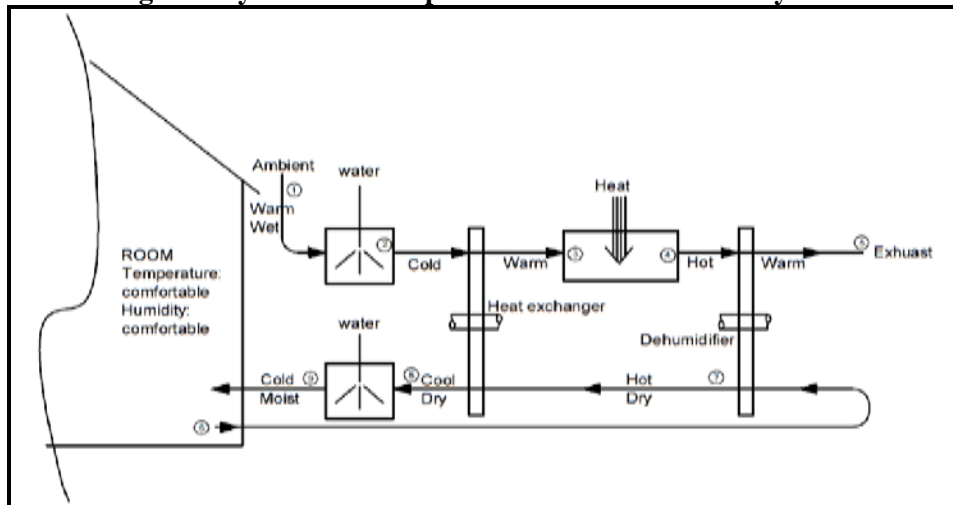**Fig.3-b Psychrometric representation of ventilation cycle.**

Fig.4-a Schematic diagram of recirculation cycle desiccant cooling system.
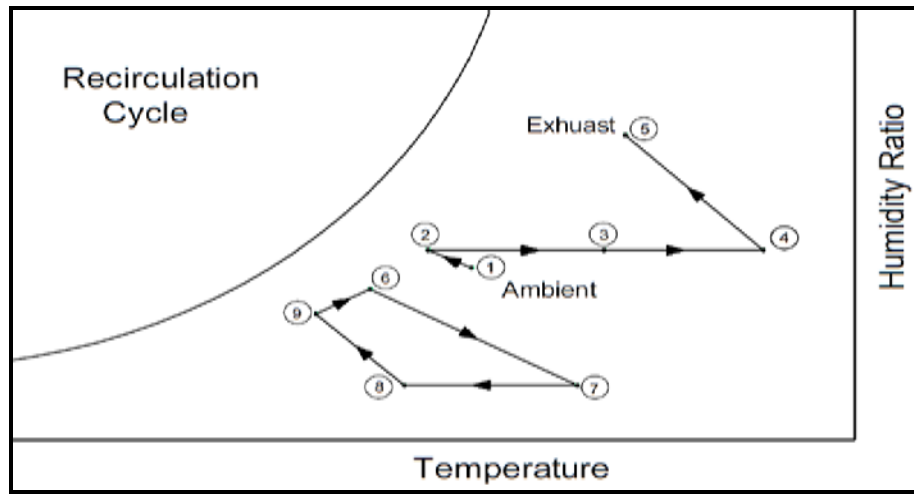
Fig.4-b Psychrometric representation of recirculation cycle.

Based on the above assumptions, the model used in this analysis is transient and one-dimensional. **Nia et.al. [2006]** estimate the outlet temperature of air by simulation as a function of $(N, T_i, d_t, T_R, w_i, D_h, U)$:

$$T_{out} = g_1(N)g_2(T_i)\,g_3(d_t)\,g_4(T_R)\,g_5(w_i)g_6(D_h)\,g_7(U)$$

(12)

$$g_1(N) = -0.0002N^2 + 0.0112N + 0.4201$$
$$g_2(T_i) = -0.0001T_i^2 + 0.0275T_i + 0.7993$$
$$g_3(d_t) = -18.79d_t^2 + 7.92d_t + 1.75$$
$$g_4(T_R) = -0.0004T_R^2 + 0.1255T_R + 0.6757$$
$$g_5(w_i) = 594.48w_i^2 + 26.76w_i + 3.79$$
$$g_6(D_h) = -0.039D_h^3 + 0.026D_h^2 + 0.603D_h + 0.0912$$
$$g_7(U) = -0.06U + 0.7973$$

Air stream dehumidification occurring in desiccant wheel and its operation can be considered by combination of its heat and mass transfer. Combination of these two processes introduces different definitions of desiccant wheel's effectiveness. The definition by using the humidity ratio given by **Steich [1994]** is adopted:

$$\varepsilon = \frac{w_{inlet\,air} - w_{outlet\,air}}{w_{inlet\,air}}$$

(13)

The effectiveness of desiccant is computed as a function of $(N, T_i, d_t, T_R, w_i, D_h, U)$:

$$\varepsilon = f_1(N)\,f_2(T_i)f_3(d_t)\,f_4(T_R)\,f_5(w_i)f_6(D_h)f_7(U)$$

(14)

$$f_1(N) = -0.0001N^2 + 0.0042N + 0.4474$$
$$f_2(T_i) = -0.0001T_i^2 - 0.0031T_i + 0.8353$$
$$f_3(d_t) = -21.67d_t^2 + 6.93d_t + 1.34$$
$$f_4(T_R) = -0.0001T_R^2 + 0.0355T_R - 0.04924$$
$$f_5(w_i) = 592.77w_i^2 - 41.23w_i + 1.283$$
$$f_6(D_h) = -.0572D_h^3 + 0.0933D_h^2 + 0.6139D_h - 0.0922$$
$$f_7(U) = -0.0611U + 0.8376$$

The sensible cooling for the dehumidified process air in this work is accomplished by a water-cooled cross flow heat exchanger. The outlet state of the process air from the heat exchanger is calculated using the usual heat exchanger effectiveness correlation given by **Moneer [1997]**:

$$T_{p,o} = T_{p,i} + \varepsilon_{hx}(T_{w,i} - T_{p,i})$$

(15)

The state of inlet process air is assumed uniform at the bulk mean outlet state of the previous upstream component. In addition, the moisture content of the process air through the heat exchanger is assumed constant because no mass transfer occurs here. The temperature of the cooled water entering the heat exchanger was assumed equal to 3 ^{o}C greater than the wet

bulb of the ambient air. This was done in order to obtain more factual condition of water and process air in case a cooling tower is used in large-scale applications to provide cooling water for the heat exchanger.

The evaporative cooler was modeled by a simple effectiveness correlation. The effectiveness of the evaporative cooler was defined by **Stoecker and Jones [1982]** as the decrease in the dry bulb temperature during evaporative cooling, divided by the wet bulb depression of entering air. The dry bulb temperature of the process air leaving the evaporative cooler is then calculated from:

$$T_{db,o} = T_{db,i} - \varepsilon_{ev}(T_{db,i} - T_{wb,i}) \qquad (16)$$

The wet bulb temperature of process air entering the evaporative cooler is calculated as a function of the dry bulb temperature and moisture content of the process air from the following empirical relation.

$$T_{wb,i} = 2.265 * \sqrt{1.97 + 4.3 T_{db,i} + 10000\, w_i} - 14.85 \qquad (17)$$

2.5 Overall System Performance:

The efficiency of a desiccant cooling system is usually expressed in terms of two important parameters. These parameters are the cooling capacity and the coefficient of performance COP. The cooling capacity of the process air supplied by the system is usually defined as the difference in enthalpy between the supply air and any given interior condition. However, it should be pointed out that the actual cooling capacity in this system is only sensible. Moisture generated within the space is inadvertently picked up by the cool air rather than removed as in the normal workings of mechanical air conditioners. It cannot be truly said that evaporative coolers remove latent heat. This is particularly true in the ventilation mode. **Joudi and Madhi [1987]** indicated that the sensible cooling capacity based on temperature difference is more factual than calculating it based on enthalpy difference. Thus, the cooling capacity of the current system was calculated as:

$$CC = \dot{m}\, C_p\, (T_R - T_S) \qquad (18)$$

In this work, the coefficient of performance was evaluated using the expression suggested by **Joudi and Madhi [1987]** who defined the COP of these systems as the heat removed from the process air stream divided by energy input to the cycle. Energy input includes electric energy to circulate air, water and rotating the desiccant wheel. Solar energy is considered free. On this basis, the coefficient of performance is:

$$COP = \frac{RE}{EP} \qquad (19)$$

Where, $RE = \dot{m}_p (h_1 - h_4)$

EP = electrical power input to the cycle

The enthalpy of the process air at various states was calculated, as a function of the dry bulb temperature and moisture content at these states, from the following empirical relation:

$$h_N = 1.005 T_N + (2467 + 1.407\, T_N)\, W_N \qquad (20)$$

2.6 Load Matching:

Most air conditioning systems, meet the variable cooling load of a space either by a variable supply temperature, keeping a constant air volume flow rate, or a variable air volume (VAV) with a constant supply air temperature.
The (VAV) control method will be applied by determining the supply air quantity required to meet the room cooling load from an energy balance between the supply air and room air:

$$\dot{m}_{sp}(h_r - h_{sp}) = Q_s + Q_l \qquad (21)$$

So, supply mass flow rate may be calculated as follows:

$$\dot{m}_{sp} = \frac{Q_s + Q_l}{h_r - h_{sp}} \qquad (22)$$

In fact, the situation in the present work differs from both types. That is, neither the temperature nor the volume flow rate of the supply air is constant. The concept of VAV is applied as a control strategy, but the supply air temperature also varies due to the variation in ambient and system operating conditions. However, from the control stand points, this uncontrolled variation in supply temperature,

above a design value, may be considered analogous to an extra cooling load, giving rise to the space air temperature in an actual VAV system.

3. RESULTS AND DISCUSSION:

3.1 Factors Affecting Cooling Load:

Fig.5-a shows the hourly variation of total cooling load and its components in July for the meeting hall with Iraqi specifications. While **Fig.5-b** shows the cooling load and its components for the same meeting hall but with the ASHRAE specifications. It can be seen that the cooling load for the Iraqi specifications is 8 % larger than that of ASHREA because of the heavy insulating coating in the wall of ASHRAE specifications.

3.2 System Component Performance:

It is known that system performance is mainly governed by the design and operating parameters of its components. The solar assisted desiccant cooling system is investigated and discussed through the analysis of performance of its components by a simulation program.
The maximum outlet temperatures occur at 14 p.m and the ambient temperature occur at 15 p.m. This is due to the variation of thermal losses from collector during the day. **Fig.6** shows the variation of the outlet temperature for various flow rates. It is observed that the temperature varies inversely with flow rate. This is due to the fact that increasing the mass flow rate leads to a lower temperature level of operation. When the flow rate decreased by 50 % the temperature increased by 11 % and when the flow rate decreased by   33 %   the temperature increased 25 % .

The performance of the desiccant wheel is measured by the outlet humidity ratio w_o of the air in both regeneration and adsorption processes. In the regeneration process, high values of w_o is an indication of a good regeneration process of the silica gel, while low values of w_o for the process is a measure of the good quality of the dehumidified air during the adsorption process. **Fig. 7** shows the reduction in moisture content with regeneration temperature for various rotational speeds of the desiccant wheel. It seen that the reduction in moisture content increases when the regeneration temperatures increase. Increasing the

regeneration temperature increases the ability of the desiccant to adsorb more moisture from air.

Fig.8 the effectiveness vs. the regeneration temperature for 54 , 48 and 24 ^{o}C ambient temperatures, it seen that the effectiveness increased by 12.7 % , 15.1 % and 21 % respectively with increasing in regeneration temperature from 60 ^{o}C to 90 ^{o}C for ambient temperature stated. **Fig.9** show the effect of regeneration temperature on the effectiveness of dehumidifier for 10 , 20 and 30 rph with increasing ambient temperature during hour of day. It seen for all rotational speed the effectiveness increased until the regeneration temperature reach 50°C   then it decreased. This is because the capacity of silica gel to adsorb the moisture from the air decreases with the increasing of ambient temperature so the reduction in moisture content decreased.

Fig.10 shows the effect of ambient temperature (process air inlet temperature) on the reduction of moisture content for various regeneration temperatures. For a 60 ^{o}C , 70 ^{o}C , 80 ^{o}C and 90 ^{o}C regeneration temperature the reduction in moisture content decreased by 32 %, 30.6 %, 31 % and 32.2 % respectively when ambient temperature increased from 13 ^{o}C to 55 ^{o}C during the day selected.

Fig.11 shows the effect of ambient temperature on the effectiveness for various regeneration temperatures. The effectiveness increased with the increasing in regeneration temperature for a constant ambient temperature.

The effect of ambient temperature (process air inlet temperature) on the outlet process air temperature is shown in **Fig.12**. It is known that when the silica gel adsorbs moisture from process air, heat of adsorption is liberated and transferred to the process air stream which increases its temperature.

In this work the heat exchanger was assumed to have a constant effectiveness of 0.9 .**Fig.13** shows the variation of supply air temperature with local time for various inlet water temperature to the heat exchanger. **Joudi and Dhaidan [2001]** assumed the water temperature entering the heat exchanger to be higher than the wet bulb temperature of the ambient air by 3 ^{o}C . The supply air temperature is still effective to present the comfort space conditions even though the water temperature may be as high as 10 ^{o}C higher than the wet bulb temperature .

Fig.14 shows the effect of effectiveness on the moisture content of the supply air during the

hours of the day selected. It shows that when the effectiveness increased by 10 % the change in moisture content is not significant but it affects the supply air temperature by 22 % in mid day. This effect is shown in **Fig. 15**.

3.3 The solar cooling system performance:

Fig.16 shows the sensible cooling load vs. the VAV mass flow rate for 4 hour occupation and 4 modes of operation. The increasing in sensible cooling load from 13500 W to 19300 W led to an increase in the flow rate by 80 % for ventilation and 64.2 % , 55.7 % , 43.4 % at 30 % , 60 % and 100 % recirculation for recirculation modes respectively. The largest increase occurred when the system operate in the ventilation mode, because of the operation of system in ventilation mode need a high cooling capacity, therefore, the flow rate increased.

Fig. 17 shows effect of the operation mode on the supply air temperature with increasing sensible cooling load. We can see that when the sensible cooling load increased by 43 % the supply temperature increased from 12 ^{o}C to 14.4 ^{o}C ventilation mode and from 11 ^{o}C to 12.5 ^{o}C for 100 % recirculation mode.

The effect of the regeneration temperature on the supply temperature for 4 operation modes is shown in **Fig.18**. The increasing in the regeneration temperature increases the supply temperature because increased the heat transfer to the process air stream.

Fig.19 shows the effect of various operation modes on the moisture content with local time. The low moisture content occurred in the 100 % recirculation mode which refers to best case for removing latent cooling load. But for the meeting room the fresh air is needed only to preserve the air quality recommended by ASHRAE. Therefore, the 30 % recirculation mode of operation is appropriate.

Fig.20 shows the variation of COP with local time for 4 operation modes. The profile of the COP is the same of the cooling load profile, because the mass flow rate in the VAV system varies as the cooling load varies during the day and the power consumption by the system is constant so that the COP profiles follow the cooling load profile. Also, the higher COP is seen to be in the ventilation mode of operation because the refrigeration effect in this mode is highest as it cools the ambient temperature to the supply temperature.

4. CONCLUTIONS:

From the results obtained for the cooling load calculations and system performance simulation, the following conclusion can be made:

1. The desiccant cooling system can supply air at temperatures ranging from 10°C to 17 ^{o}C with low moisture content with the ability to remove sensible and latent heats from the conditioned space.

2. A regeneration temperature ranging from 55 ^{o}C to 75 ^{o}C was obtained from the solar air heater giving a dehumidifier effectiveness of 45 % and 55 % .

3. The ranging of rotational speed of desiccant wheel from 10 rpm to 30 rpm don't affect the reduction in moisture content and the effectiveness of the dehumidifier.

4. The performance of the desiccant cooling system is more influenced by the effectiveness of the heat exchanger and evaporative cooler and also by the regeneration temperature

5. The COP profile follows the same trend as the cooling load profile. COP ranged from 0.5 to 12. Its highest at ventilation modes.

6. The system operation mode with 30 % recirculation air is adequate and reliable for providing comfort air conditioning for the meeting hall.

REFERENCES

ASHRAE Handbook of Fundamental, American society for Heating, Refrigeration and Air Conditioning Engineers, Inc., New York,(2009).

Ammari HD. A mathematical model of thermal performance of solar air heater with slats. Renewable Energy 2003; 28: 1597-1615.

Camargo JR, Ebinuma CD, Silveira JL. Experimental performance of a direct evaporative cooler operating during summer in a Brazilian city. International Journal of Refrigeration 2005; 28:1124-1132.

Daou K, Wang RZ, Xia ZZ. Desiccant cooling air conditioning: a review. Renewable and Sustainable Energy Reviews 2006;10: 55-77.

Datta S, Sahgal PN, Subrahamaniyam S, Dhingra SC, Kishore VV, Design and operating characteristics of evaporative cooling systems. International Journal of Refrigeration 1987; 10(7):205-208.

Duffie JA and Beckman WA, Solar Engineering and Thermal Process, John Wiley and Sons, New York, (2006).

El-Dessouky H, Ettouney H, Al-Zeefari A. Performance analysis of two-stage evaporative coolers. Chemical Engineering Journal 2004; 102: 255-266.

Heidarinejad G, Bozorgmehr M, Delfani S, Esmaeelian J. Experimental investigation of two-stage indirect/direct evaporative cooling system in various climatic conditions. Journal of Building and Environment 2009; 44:2073-2079.

Joudi KA, Dhaidan NS. Application of solar assisted heating and desiccant cooling systems for a domestic building. Energy Conversion and Management 2001; 42:995-1022.

Joudi KA, Madhi SM. An experimental investigation into solar assisted desiccant-evaporative air conditioning system. Solar Energy 1987; 39(2): 97-107.

Joudi KA, Mehdi SM. Application of indirect evaporative cooling to variable domestic cooling load. Energy Conversion and Management 2000; 41:1931-1951

Kodama A, Hirayama T, Goto M, Hirose T, Critoph RE. The use of psychrometric charts for the optimization of thermal swing desiccant wheel. Applied Thermal Engineering 2001; 21:1657-1674.

Mittal MK, Varun, Saini RP, Singal SK. Effective efficiency of solar air heaters having different types of roughness elements on the absorber plate. Energy 2007; 32: 739-745.

Mohammad AI. An investigation in to solar assisted evaporative cooling system, M.Sc. Thesis, university of Basrah, Basrah,(1983).

Moneer AK. A preliminary computer simulation of an open solar assisted desiccant cooling system, M.Sc. Thesis, university of Baghdad, Baghdad,(1997).

Nia FE, van Paassen D, Saidi MH. Modeling and simulation of desiccant wheel for air conditioning. Energy and Buildings 2006; 38:1230-1239.

Steich G. Performance of rotary enthalpy exchanger. M.Sc. Thesis in Mechanical Engineering, University of Wisconsin-Madison, 1994.

Stoecker WF, Jones JW. Refrigeration and Air Conditioning, McGraw-Hill Pub. Co., New York, (1982).

Urban RA. Design considerations and operating characteristics of variable volume systems. ASHRAE Journal 1969; 12 (2): 77–84.

Varun, Saini RP, Singal SK. A review on roughness geometry in solar air heaters. Solar Energy 2007; 81:1340-1350.

Zhang XJ, Dai YJ, Wang RZ. A simulation study of heat and mass transfer in a honeycombed rotary desiccant dehumidifier. Applied Thermal Engineering 2003; 23:989-1003.

Nomenclature

Symbol	meaning	Units
A	Area	m^2
C_p	Specific heat of air	$J/kg.^oC$
CC	Cooling capacity	W
COP	Coefficient of performance	
c_0,c_1..etc	Conduction time factors	
D_h	Hydraulic diameter of a channel	m
d_t	Thickness of the desiccant coating	m

F_R Heat removal factor

F' Collector efficiency factor

G Mass flow rate per unit area of collector $kg/s.m^2$

I Irradiance W/m^2

$IAC(\theta,\Omega)$ Indoor solar attenuation coefficient for beam solar heat gain coefficient

IAC_D Indoor solar attenuation coefficient for diffuse solar heat gain coefficient

h_o Coefficient of heat transfer $W/m^2.K$

$\dot{m}$ Mass flow rate   kg/s

N Wheel speed   rph

     No. of day selected

q Heat gain W/m^2

Q Cooling load   W

r_o, r_1..etc   Radiant time factors

RH Relative humidity   %

W Moisture content of air   kg/kg dry air

R Long-wave radiation W/m^2

$SHGC(\theta)$ Beam solar heat gain coefficient as a function of incident angle θ

$<SHGC>_D$ Diffuse solar heat gain coefficient

S Absorbed solar radiation W/m^2

T Temperature   °C

U Overall heat transfer coefficient $W/m^2.K$

Subscripts:

a   ambient

b   beam

c   convective

d   diffuse

l   latent

p   plate/process air

s   supply/sensible

sol   sol-air temperature

r   room/reflected/regeneration

t   total

Greek symbol

θ angle of incidence/hour

η efficiency

ε effectiveness
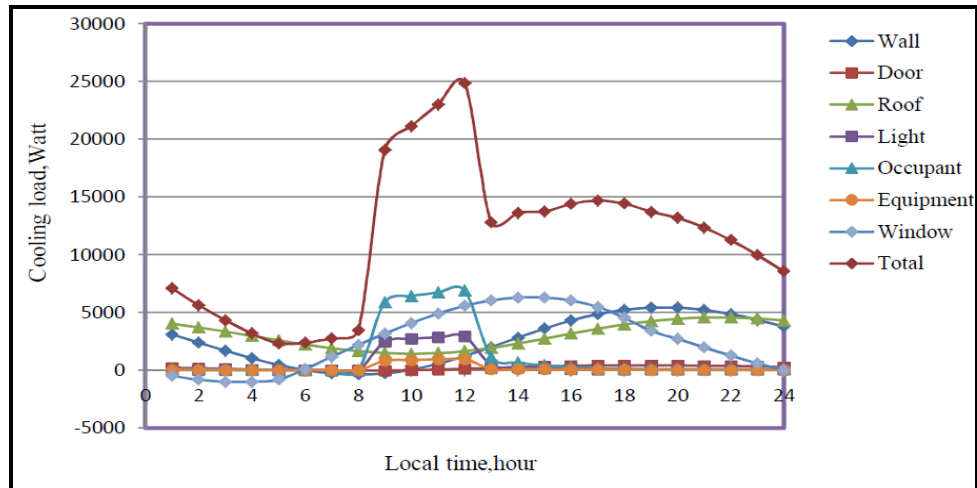
**Fig.5-a Hourly variation of cooling load components with local time 4-hour occupation
on 21 July. Iraqi specification.**
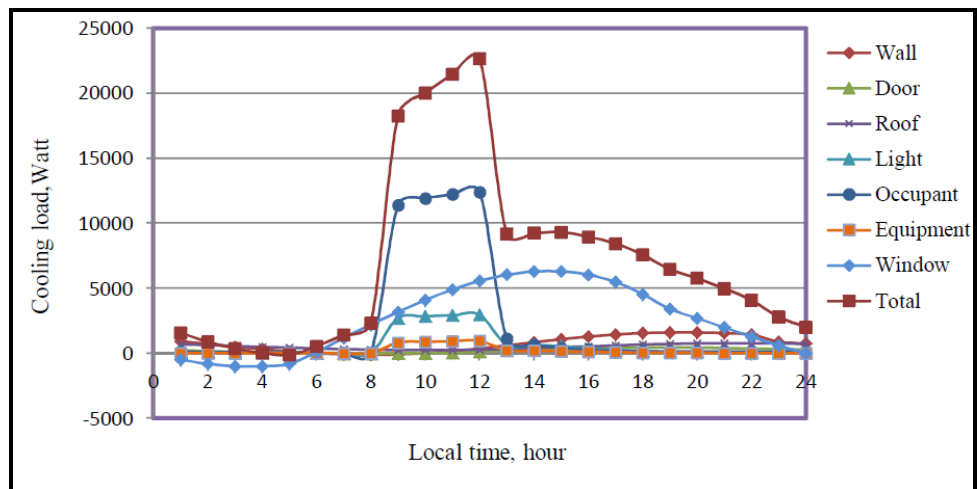
**Fig.5-b Hourly variation of cooling load components with local time 4-hour occupation
on 21 July. ASHRAE specification**
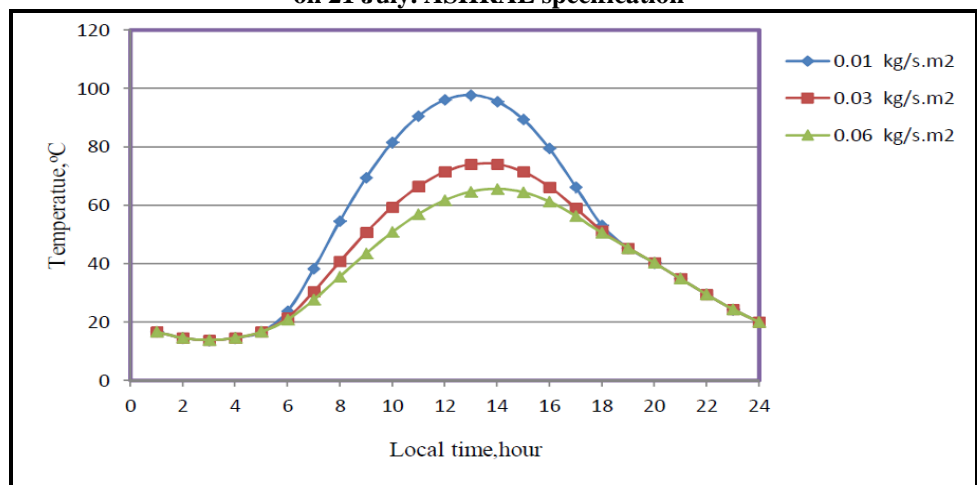
**Fig.6 Hourly variation of outlet temperature from solar collector with local time
for various flow rates**

1613
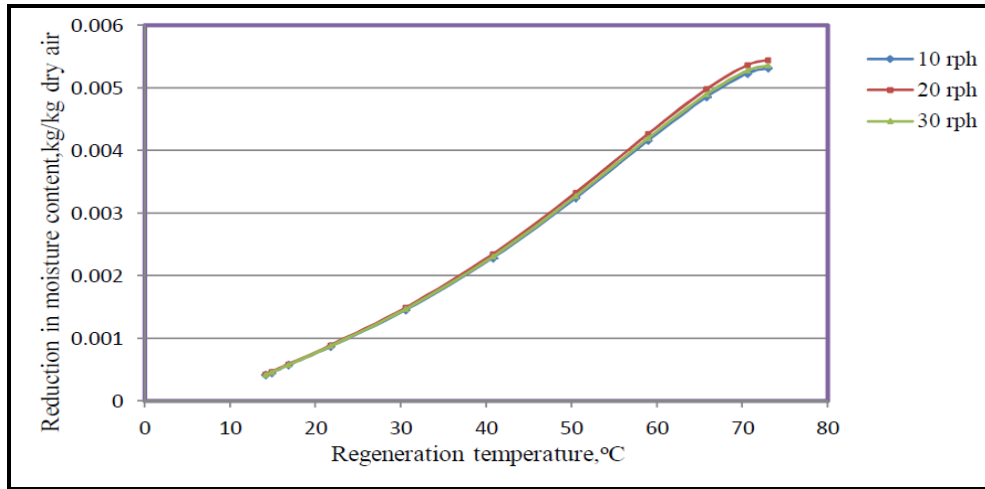
Fig.7 Effect of regeneration temperature on the reduction in moisture content for various rotational speeds of desiccant wheel
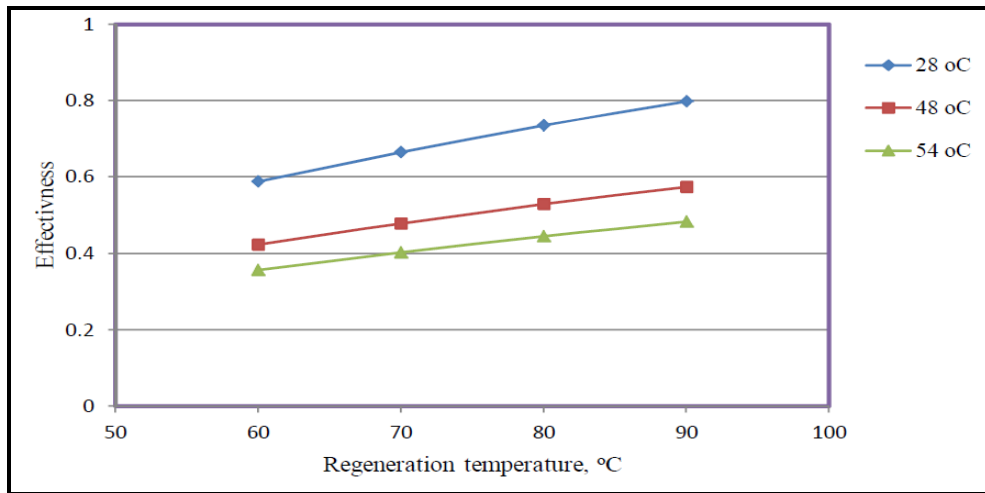
Fig.8 Effect of regeneration temperature on the effectiveness for various ambient temperatures
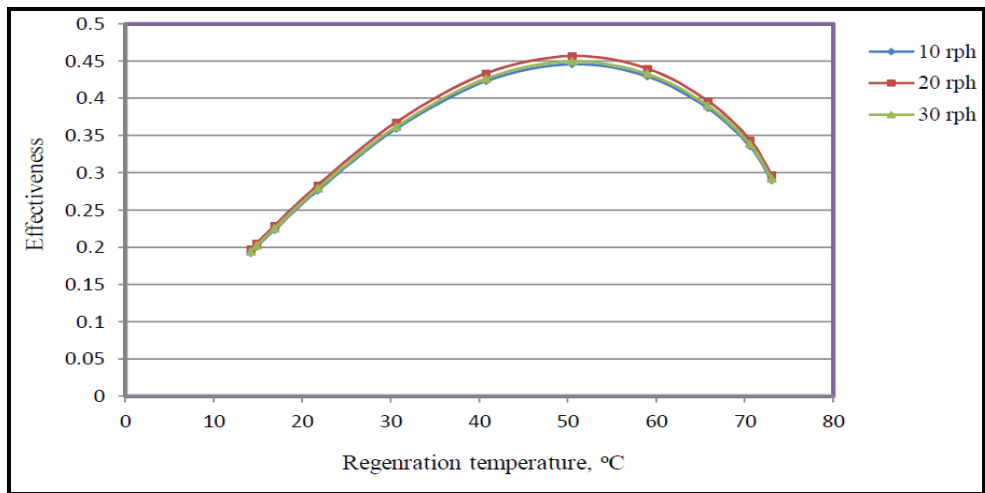
Fig.9 Effect of regeneration temperature on effectiveness of desiccant wheel for various rotational speeds
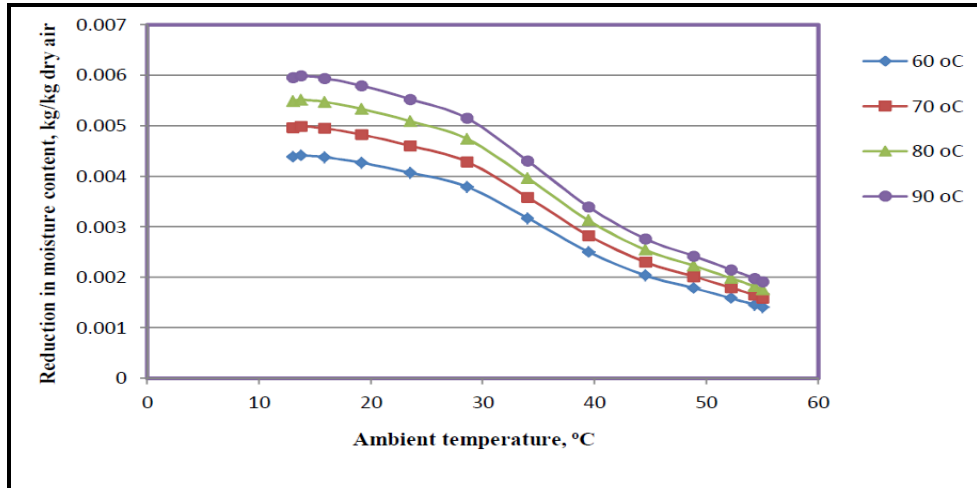
Fig. 10 Effect of ambient temperature on the reduction in moisture content for various regeneration temperatures
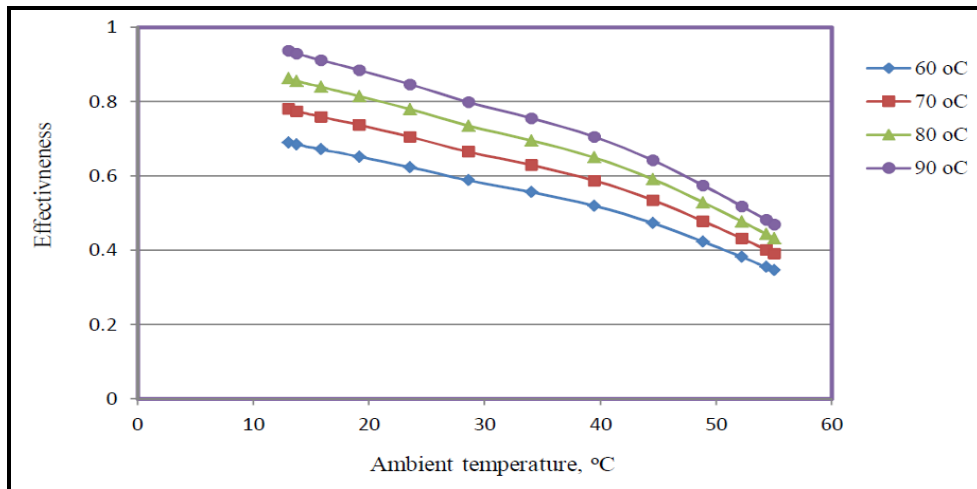
Fig.11 Variation of effectiveness with ambient temperature for various regeneration temperatures
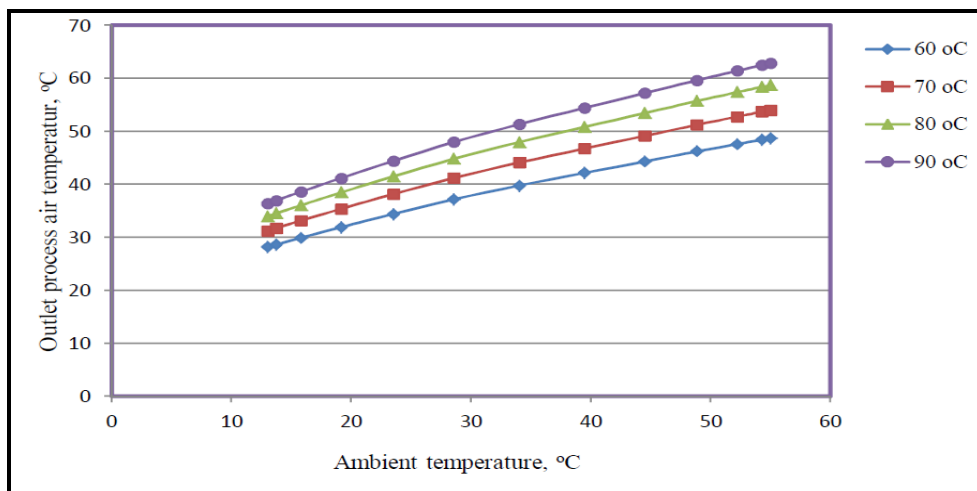
Fig.12 Variation of outlet air temperature from desiccant wheel with ambient temperature for various regeneration temperatures
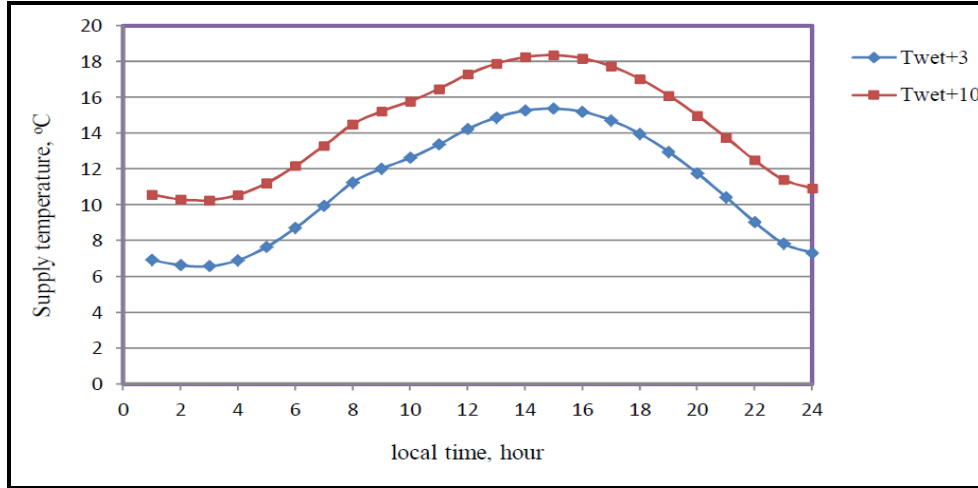
Fig.13 Variation of supply air temperature with local time for various inlet water temperature of heat exchanger, η_{hx}= 0.9
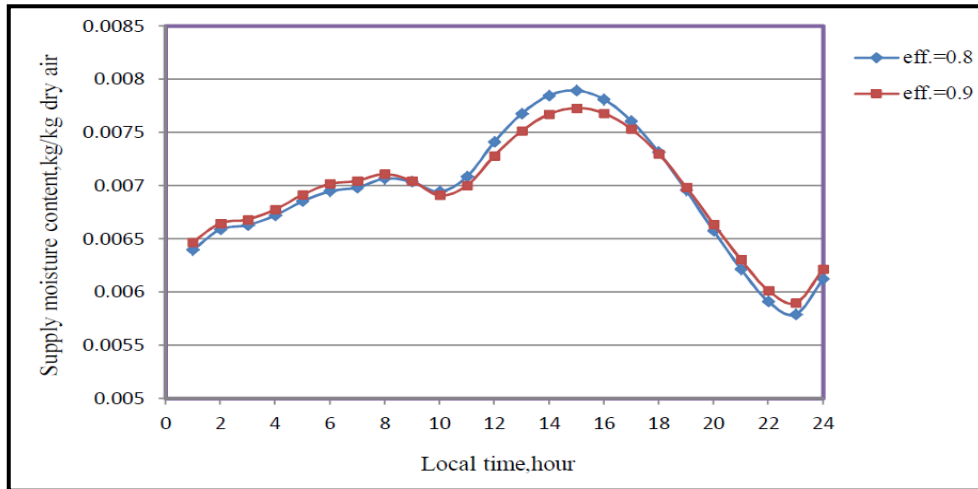
Fig.14 Variation of supply moisture content with local time for various evaporative cooler effectiveness
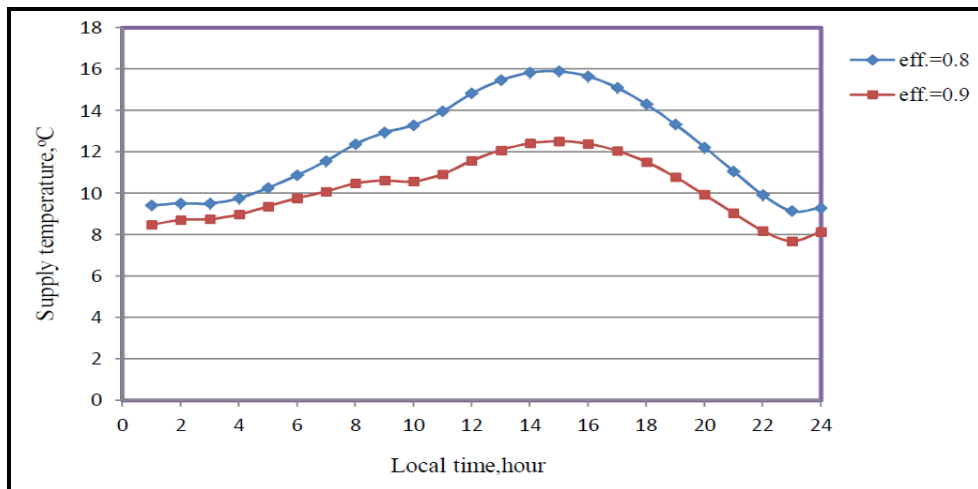
Fig..15 Action of supply air temperature for various effectiveness of evaporative cooler with local time
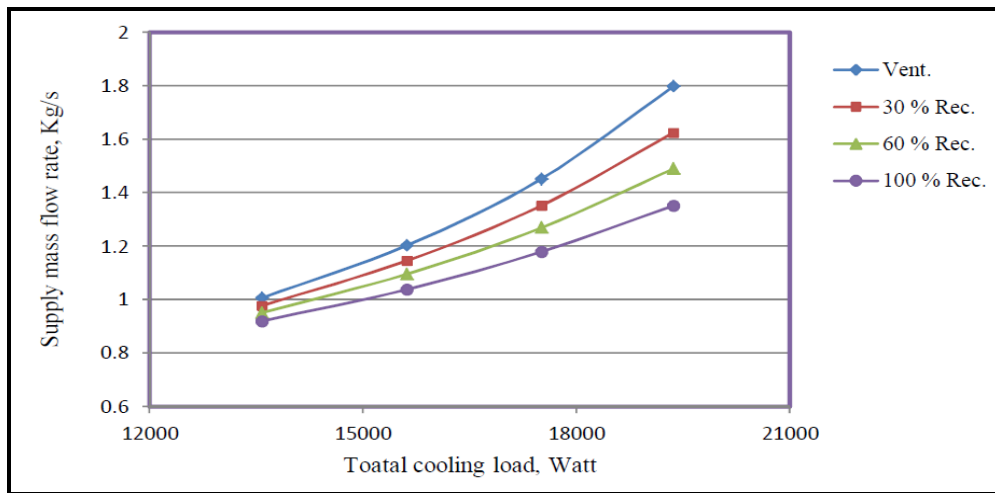
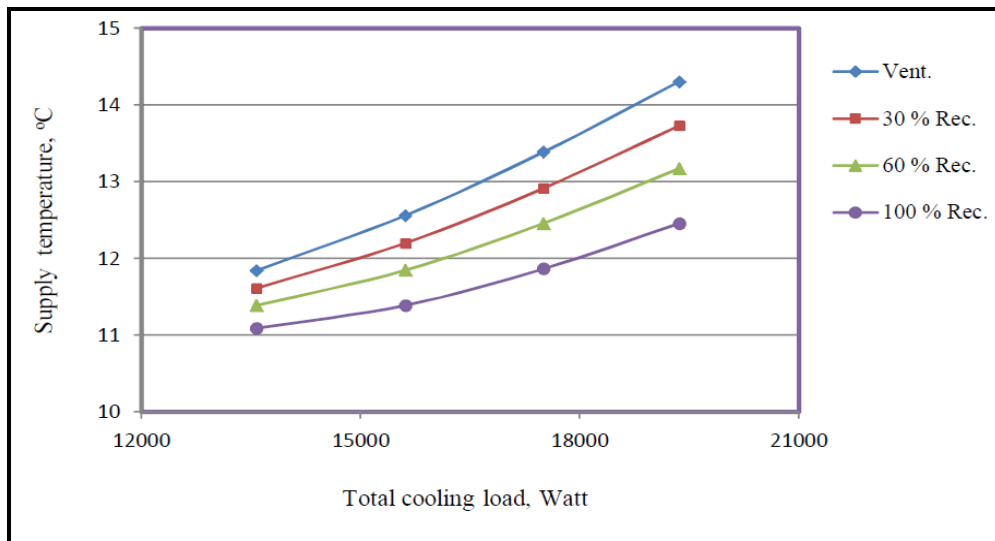**Fig.16 Variation of supply air mass flow rate with total cooling load for various operation modes**

Fig.17 Variation of supply air temperature with total cooling load for various operation modes
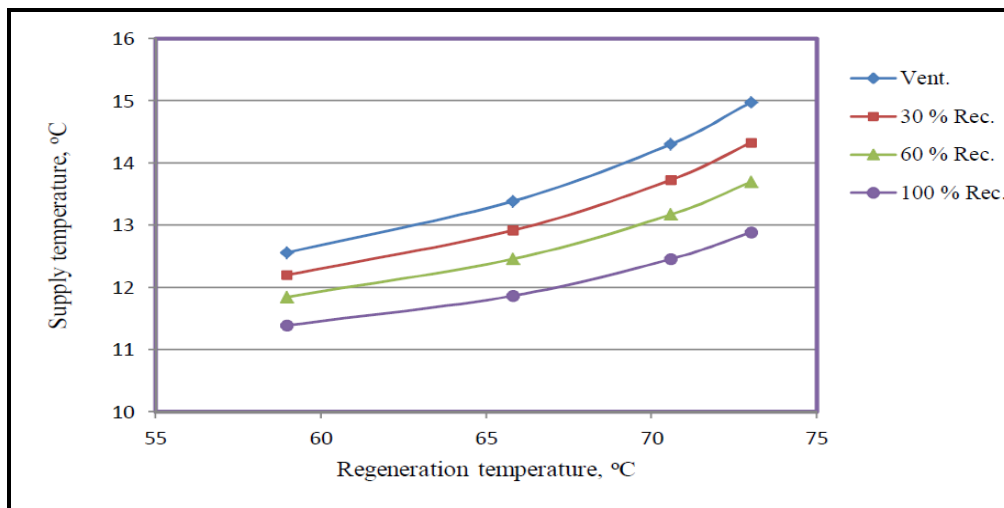

Fig.18 Effect of regeneration temperature on supply temperature for various operation modes
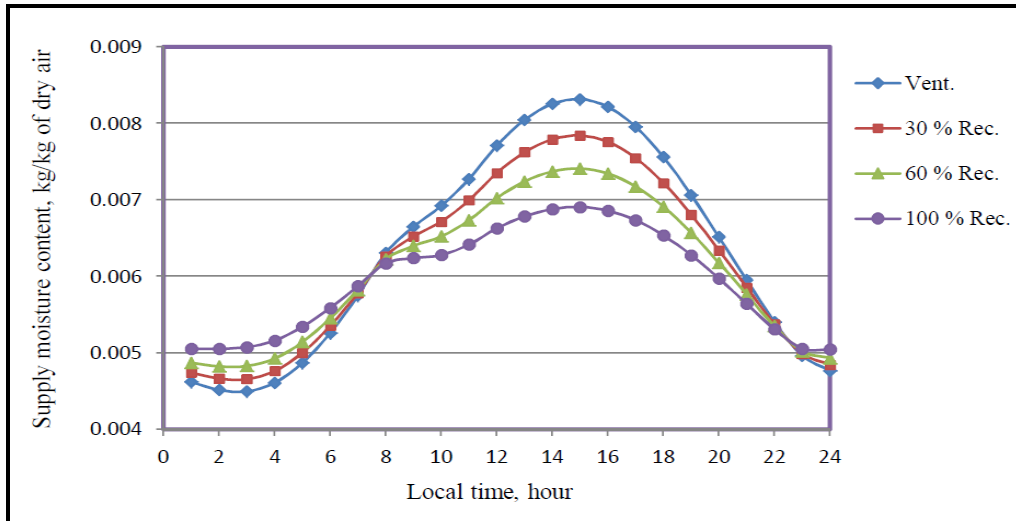
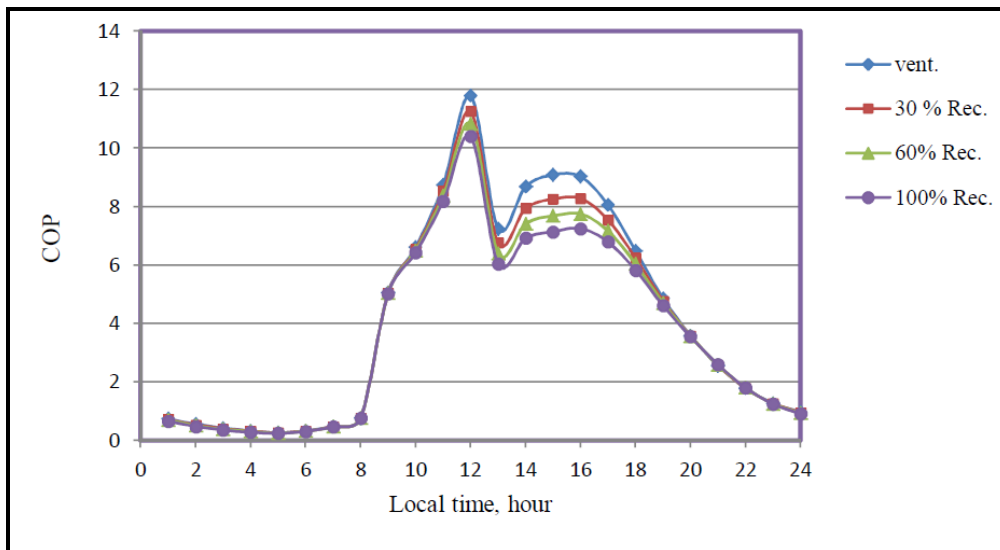**Fig.19 Effect of operation modes on the supply moisture content with local time**

Fig.20 Effect of operation modes on the COP with local time